Road Materials and Pavement Design

ISSN: 1468-0629 (Print) 2164-7402 (Online) Journal homepage: www.tandfonline.com/journals/trmp20

Characterising the resilient behaviour of unsaturated sandy soils under suction-controlled tests

José H. C. Everton & Sigurdur Erlingsson

To cite this article: José H. C. Everton & Sigurdur Erlingsson (07 Apr 2025): Characterising the resilient behaviour of unsaturated sandy soils under suction-controlled tests, Road Materials and Pavement Design, DOI: 10.1080/14680629.2025.2480249

To link to this article: https://doi.org/10.1080/14680629.2025.2480249

Published online: 07 Apr 2025.

ROAD MATERIALS AND PAVEMENT DESIGN
https://doi.org/10.1080/14680629.2025.2480249

Taylor & Francis
Taylor & Francis Group

Characterising the resilient behaviour of unsaturated sandy soils under suction-controlled tests

José H. C. Everton[a,b] and Sigurdur Erlingsson[a,b,c]

[a]Pavement Technology, Swedish National Road and Transport Research Institute, Linköping, Sweden; [b]Department of Civil and Architectural Engineering, Royal Institute of Technology, Stockholm, Sweden; [c]Faculty of Civil and Environmental Engineering, University of Iceland, Reykjavik, Iceland

ABSTRACT

This study investigates the influence of moisture and suction on the resilient modulus (M_R) of subgrade soils. The research employs suction-controlled Repeated Load Triaxial (RLT) tests on three sandy materials with varying fines content. The soil water retention curves (SWRC) for the three materials were obtained and allowed expediting suction equilibrium outside the triaxial chamber by controlling the water loss and thus inferring the yielded suction with the SWRC parameters. The results show that M_R increases with lower moisture content and higher suction. Two stress-based models and two moisture-based models are evaluated for predicting M_R. The findings indicate that stress-suction models provide a good fit for the silty sands, but only the model where suction is an independent variable suits all tested materials. Additionally, a proposed suction-based model demonstrates promising results. Overall, the study highlights the importance of considering both moisture and suction for accurate M_R characterisation of subgrade soils.

ARTICLE HISTORY
Received 6 September 2024
Accepted 10 March 2025

KEYWORDS
Subgrade soils; resilient modulus; moisture content; suction; repeated load triaxial testing; soil water retention curve

Introduction

The subgrade, as the foundation of pavement structures, is important for providing stability during the construction of the pavement layers and for the sound operation of roads, withstanding traffic loads and seasonal variations. However, the subgrade is often the weakest part of the pavement, and is also subject to softening processes due to environmental conditions such as freeze and thaw (F-T) (Doré & Zubeck, 2009), wet and dry (W-D) (Rasul et al., 2018) and excessive rutting due to heavy traffic loading (Erlingsson, 2012). Therefore, it is important to know the mechanical properties of subgrade soils to properly address these issues in pavement design and predict pavement performances as a function of time.

The upper part of the subgrade is typically compacted at conditions close to their optimum moisture content (OMC), which enhances its mechanical properties by increasing its dry density (Huang, 2004). As subgrade soils are subjected to wetting and drying, their equilibrium moisture can be on either wet or dry of the optimum (Zapata, 2018). This equilibrium moisture can change during and between seasons, hence the importance of testing the material at different moisture-suction levels to get a full picture of the material's stiffness (Cary & Zapata, 2011; Han & Vanapalli, 2015; Lekarp et al., 2000). Suction in subgrades soils is characterised by water in tension within the particle's menisci, which in effect enhances the material's cohesion (Fredlund et al., 1978). An increase in suction is observed with a decrease in water content.

CONTACT José H. C. Everton josece@kth.se

It has been established that the upper part of a pavement subgrade will be unsaturated for most of its design life (Han & Vanapalli, 2015). The subgrade can be expected to retain some contact with the atmosphere, and therefore to lose moisture due to evaporation and to gain it due to rising groundwater levels and/or precipitation. As the subgrade dries and suction increases it can be expected to present gains in strength and stiffness, while wetting can trigger softening and loss of stiffness (Blackmore et al., 2020).

The measure of stiffness for subgrades is referred to as the Resilient Modulus (M_R) (Equation 1), which reflects on the resilient or recoverable strain ε_r that the subgrade shows when cyclically loaded under a deviatoric stress $\sigma_d = \sigma_1 - \sigma_3$.

$$M_R = \frac{\sigma_d}{\varepsilon_r} \tag{1}$$

Repeated Load Triaxial (RLT) tests conducted to characterise the M_R of subgrades have shown their sensitivity to moisture and their nonlinearity to stress levels (Lekarp et al., 2000). For fine-grained subgrades, however, previous studies have shown that models based on suction yield better predictions of M_R than models based on moisture content (Cary & Zapata, 2011).

Although the fact that M_R varies with suction levels has been described in previous studies (Han & Vanapalli, 2015; Ng et al., 2013; Salour & Erlingsson, 2015), there are different interpretations regarding the magnitude of this variation (Liang et al., 2008). Hence models using suction for predicting M_R can be divided into two groups: those that consider suction as an independent variable (Cary & Zapata, 2011; Ng et al., 2013; Zhang et al., 2020, 2021) and those that consider it as a contributor to the average skeleton stress (Liang et al., 2008; Park et al., 2024).

This study attempts to model the resilient behaviour of sandy soils with different gradations, whereby experimental data from suction-controlled RLT tests associated with soil water characteristic tests were used to evaluate two stress-based models including suction, proposing improvements where appropriate. Furthermore, as the state of practice is still reliant on the influence of the moisture content separately from the influence of stress state in what is known as the Mechanistic Empirical Pavement Design Guide (MEPDG) moisture-based model (ARA, 2004), a simple suction-based model dissociated from the stress state is proposed to be compared with the MEPDG moisture-based model.

Therefore, this study aims to improve M_R prediction models for sandy soils and as a consequence enhance pavement design using a Mechanistic-Empirical (M-E) pavement design approach by accomplishing the following objectives:

(1) To establish the relationship between moisture and suction for each material, known as Soil Water Retention Curve (SWRC).
(2) To obtain subgrade material parameters for accurate resilient modulus prediction models based on RLT test data, checking their goodness of fit and if needed, to modify and propose new resilient modulus prediction models, checking their goodness of fit and comparing with the previous models.

Effective stress in unsaturated subgrades

There have been different interpretations regarding the role of suction in the stress state of unsaturated soils. For some, two independent stress variables govern the mechanical properties of unsaturated soils: a net mean normal stress σ' and a matric suction ψ_m (Fredlund & Morgenstern, 1977) (Equation 2).

$$\sigma' = \sigma - u_a, \quad \psi_m = u_a - u_w \tag{2}$$

where σ is the mean normal stress, u_a is the pore-air pressure and u_w is the pore-water pressure.

For others, suction is not an independent stress state but rather a component of the effective stress variable (Bishop, 1959; Lu & Likos, 2006). The simplified Bishop's effective stress p' (Equation 3) takes

suction into account through the Bishop's parameter χ.

$$p' = (\sigma - u_a) - \chi.(u_w - u_a) = \sigma' + \chi.\psi_m \tag{3}$$

where $0 \leq \chi < 1$ for unsaturated conditions, and $\chi = 1$ for saturated conditions. In such a case, Equation 3 equals Terzaghi's effective stress equation.

Estimating the Bishop's parameter χ is challenging due to the impractical and time-consuming laboratory tests required and the complex interdependency on soil properties and conditions, including soil pore structure and suction (Rojas, 2008). Hence researchers have proposed indirect methods to estimate χ. Amongst such indirect methods, two were suggested in existing M_R predictive models: the approach proposed by Khalili and Khabbaz (1998), which suggested a relationship between χ and matric suction (Equation 4) and the conceptual approach proposed by Lu et al. (2010) between χ and volumetric water content (Equation 5).

$$\chi = \left(\frac{\psi_{\text{AEV}}}{\psi_m}\right)^{0.55} \tag{4}$$

$$\chi = S_e = \frac{\theta - \theta_r}{\theta_s - \theta_r} \tag{5}$$

where the matric suction at the air entry value ψ_{AEV} denotes the suction at the capillary rise region, which corresponds to the height of the saturated region above the groundwater table where the pore-water pressure is below atmospheric pressure. S_e is the effective degree of saturation, which discounts the residual volumetric water content θ_r, from the volumetric water content θ and volumetric water content at saturation θ_s.

Resilient behaviour models of unsaturated soils

Amongst the alternatives to account for diverse moisture states in the resilient behaviour of subgrades are stress-based models modified to include a suction component (Cary & Zapata, 2011; Khoury et al., 2009; Liang et al., 2008; Ng et al., 2013), herein called stress-suction based models, or calibrating a stress-based model that computes M_R at OMC ($M_{R\text{opt}}$) (Witczak et al., 2000), herein called moisture-based model. For the former, the resilient response can be calculated according to in-situ stresses, applied stresses and suction, whereas for the latter, M_R will vary with the moisture content.

The second alternative is implemented in the AASHTO's MEPDG (ARA, 2004), where a modified version of the widely known Universal Model (Witczak & Uzan, 1988), a stress-based model herein identified as $M_{R\text{opt}}$ in Equation 6, is calibrated according to a factor *f(S)* relating the relative change in M_R to a relative change in the degree of saturation S (Andrei, 2003); a more complete account on such factor is given in section 3.2.

$$\begin{aligned} M_R &= f(S) \cdot M_{R\text{opt}} \\ M_{R\text{opt}} &= k_1 p_a \left(\frac{\theta_b}{p_a}\right)^{k_2} \left(\frac{\tau_{\text{oct}}}{p_a} + 1\right)^{k_3} \end{aligned} \tag{6}$$

where θ_b is the bulk stress ($\sigma_1 + \sigma_2 + \sigma_3$); τ_{oct} is the octahedral stress, which in triaxial test becomes $\sqrt{2}/3 \cdot (\sigma_1 - \sigma_3)$; p_a is a reference pressure equal to 100 kPa and k_1, k_2, k_3 are regression parameters.

Stress-suction based models

The modified Universal Model $M_{R\text{opt}}$, implemented in the MEPDG, has been proved to accurately predict the resilient behaviour of different types of soils as extensively documented in foundational publications of the MEPDG (Andrei, 2003; ARA, 2004). Building on that model, researchers have proposed revisions it to include a suction variable and thus obtaining a unique set of model parameters

capable of representing variations of M_R with suction, and consequently with moisture. Amongst the proposed revisions, which are accounted for in state-of-the-art reviews (Han & Vanapalli, 2016), the following equations (7–11) were selected in this study because of their intrinsic interpretation of the role of suction in enhancing the resilient behaviour of soils, following two groups:

Group A: Suction as an independent variable.

$$M_R = k_1 p_a \left(\frac{\theta_{\text{net}} - 3\Delta u_w}{p_a}\right)^{k_2} \left(\frac{\tau_{\text{oct}}}{p_a} + 1\right)^{k_3} \left(\frac{\psi_0 - \Delta\psi}{p_a}\right)^{k4} \tag{7}$$

$$M_R = k_1 p_a \left(\frac{\theta_b}{p_a}\right)^{k_2} \left(\frac{\tau_{\text{oct}}}{p_a} + k_4\right)^{k_3} + \alpha_1 . {\psi_m}^{\beta_1} \tag{8}$$

Group B: Suction as a contributor to the average skeleton stress

$$M_R = k_1 p_a \left(\frac{\theta_b + \chi . \psi_m}{p_a}\right)^{k_2} \left(\frac{\tau_{\text{oct}}}{p_a} + 1\right)^{k_3} \tag{9}$$

$$M_R = k_1 p_a \left(\frac{\theta_b + 3p_s}{p_a}\right)^{k_2} \left(\frac{\tau_{\text{oct}}}{p_a}\right)^{k_3} \tag{10}$$

where $\theta_{\text{net}} = \theta_b - 3u_a$ is the net bulk stress, k_1, k_2, k_3, k_4, α_1 and β_1 are regression parameters; Δu_w is the change in pore-water pressure; ψ_0 is the initial matric suction; $\Delta\psi$ is the change in matric suction, and suction stress $\sigma_s = \frac{S - S_0}{100 - S_0} \Delta\psi_m$, and S_0 is the residual degree of saturation. All stresses and M_R are given in kPa.

Models in group A have the advantage of not requiring SWRC data, simplifying experiments to RLT tests; they include Equation 7 (Cary & Zapata, 2011), which considers suction as an independent variable modified by parameter k_4, leaning on the Fredlund & Morgenstern definition of effective stress; and Equation 8 (Khoury et al., 2009) which considers suction as an independent variable whose effect is added separately to the stress-correlated ones. Cary & Zapata model necessitates a more rigorous testing apparatus than that of Khoury et al. model, capable of measuring a change in suction and in pore water pressure during cyclic loading. Furthermore, the former analysis M_R in terms of net stresses while the latter analysis in terms of total stress.

Models in group B require SWRC data, such as the AEV and S_0 to determine σ_s; they include Equation 9 (Liang et al., 2008) and Equation 10 (Park et al., 2024). While both include a suction stress variable that adds to the constraint effect given by the bulk stress, leaning on Bishop's definition of effective stress, they differ on the contribution of the suction stress component with the Park et al model correctly considering the effect of the suction stress in three dimensions.

Similar studies have found that models based on the Bishop's effective stress successfully predicted the resilient behaviour of sandy materials in addition to cohesive ones (Liang et al., 2008): – as a well-graded sand and silty sand (Park et al., 2024); and of a clayey sand (Blackmore et al., 2020), hence the motivation to evaluate the model's suitability for the sandy soils selected in this study.

Moisture-based model

Obtaining reliable test results that can be used to characterise materials according to stress-suction based models requires multiple samples and specialised equipment to control or measure suction during testing (Han & Vanapalli, 2016). In this regard, moisture-based models simplify the task of obtaining M_R at different moisture states without resorting to too many test results to grasp the variation of M_R with matric suction. This alone enhances the practicality aspect, which is important for the adoption of M-E pavement design in practice.

Equation 6 is part of the Enhanced Integrated Climatic Model (EICM)(Zapata et al., 2007) incorporated in the AASHTO's MEPDG. It assumes that the contribution of moisture is independent of the contribution of stress level to the M_R, and that stress dependency is proportional at different moisture

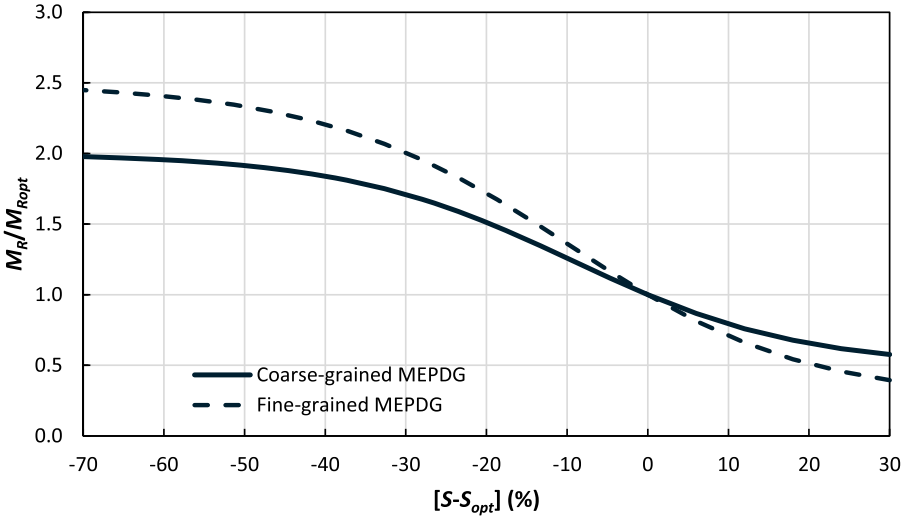

Figure 1. AASHTO's MEPDG M_R-moisture base model.

states (Andrei, 2003). On that aspect, engineering appraisal must be considered when modelling test results using such a model, as the EICM's assumption may not always be true for different materials.

Given the simplicity of the calibration factor *f(S),* widely known as the MEPDG M_R – moisture model (Andrei, 2003; ARA, 2004; Zapata et al., 2007) (Equation 11), it is one of the most widely used for predicting stiffness as moisture changes. It also has the advantage of covering both coarser-grained (typically used as base/subbase layers) and fine-grained materials (typically employed as subgrades).

$$\log[f(S)] = \log\left(\frac{M_R}{M_{\text{Ropt}}}\right) = a + \left(\frac{b-a}{1+\exp\left[\ln\left(\frac{-b}{a}\right) + k_s.(S - S_{\text{opt}})\right]}\right) \tag{11}$$

where a and b are material parameters that change with the particle size distribution, k_s is a regression parameter and S_{opt} is the degree of saturation at OMC.

The suggested values for a, b and k_m according to the literature and as implemented in the MEPDG are (ARA, 2004):

$[a, b, k_s] = [-0.3123, 0.3010, 6.8157]$ for coarse-grained soils,
$[a, b, k_s] = [-0.5934, 0.3979, 6.1324]$ for fine-grained soils.

In that model, a normalised M_R to $M_{R\text{opt}}$ (ratio of M_R) is a function of the relative change in S to S_{opt}. As can be seen in Figure 1, by plotting the model using the material parameters *a, b and* k_m according to the literature values, a sigmoidal shape is formed, which flattens out at the dry side of optimum, indicating a maximum gain in stiffness is achieved after a drop in the degree of saturation. At the wet side of optimum, a maximum loss is expected up to full saturation.

Experimental campaign

Three subgrade materials were tested in this study, one is a poorly graded sand (SP) and two are silty sands with distinct fines content (SM1 and SM2), sourced from quarries located in Jönköping and Linköping, respectively, both in southern Sweden. The materials' particle size distribution is presented in Figure 2, where SP is an open-graded sand material, SM1 and SM2 are well-graded silty sands with distinct fines content.

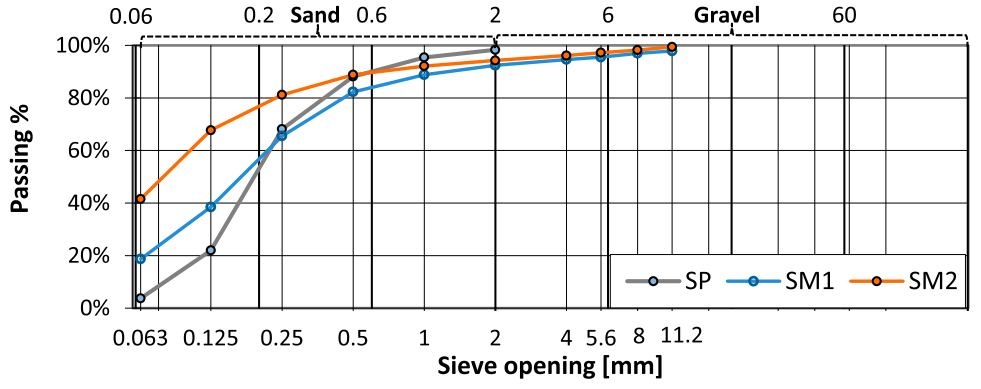

Figure 2. Particle size distrbution of selected material.

Table 1. Soil index properties.

Properties	unit	SP	SM1	SM2
Passing sieve 0.063 mm	[%]	4.0	17.4	39.0
Max. dry density ρ_d	[g/cm^3]	1.72	1.90	2.08
Grav. optimum moisture content w_{opt}	[%]	14.4	8.7	8.5
Specific gravity *Gs*	[-]	2.62	2.65	2.64
Liquid Limit	[%]	–	–	18.0
Plasticity limit	[%]	–	–	14.3
Plasticity index	[%]	NP	NP	3.7

In order to establish relationships between variations of the M_R with applied stresses, suction and moisture content, an experimental campaign focusing on suction-controlled RLT tests was executed. The campaign consisted of two phases, preceded by a preliminary step entailing the establishment of index properties, which can be seen in Table 1; the 1st phase consisted of estimating the SWRC of each material; and the 2nd phase consisted of conducting suction-controlled RLT tests for M_R on samples prepared at similar dry densities but different post-compaction moisture changes.

SWRC estimation

In order to consider the effects of suction in RLT tests it is important to first establish the subgrade's Soil Water Retention Curve (SWRC), which is the relationship between suction yielded in the material and its moisture content (Fredlund & Morgenstern, 1977). As the SWRC varies widely between different types of soil, obtaining such a relationship helps in designing suction-controlled RLT tests according to the range of suction that the material yields at different moisture contents (Salour & Erlingsson, 2015).

The SWRC was established on samples compacted in a metal ring ($h = 32$ mm, $d = 51$ mm), as seen in Figure 3(a and b), to the modified Proctor energy (2,7 MJ/m^3), using a rammer compactor for small samples (Figure 3(c)) (Walshire et al., 2019). The tests were carried out on a pressure plate apparatus known as SWC–150 from GCTS Laboratories that determines the moisture-suction relationship of each material (Figure 3(d)).

To determine the soil's main drying curve (MDC), samples were prepared at optimum moisture content and desorption tests were performed. Based on the findings of a previous study (Everton et al., 2022), the model that provided the best fit for the moisture-suction relationship for the selected subgrades was the Fredlund & Xing model (Equation 12) (Fredlund & Xing, 1994):

$$\theta(\psi) = C(\psi) \cdot \frac{\theta_s}{[\ln(e + (\psi_m/a_f)^{n_f}]^{m_f}}, C(\psi) = 1 - \frac{\ln[1 + (\psi_m/\psi_r)]}{\ln[1 + (10^6/\psi_r)]} \tag{12}$$

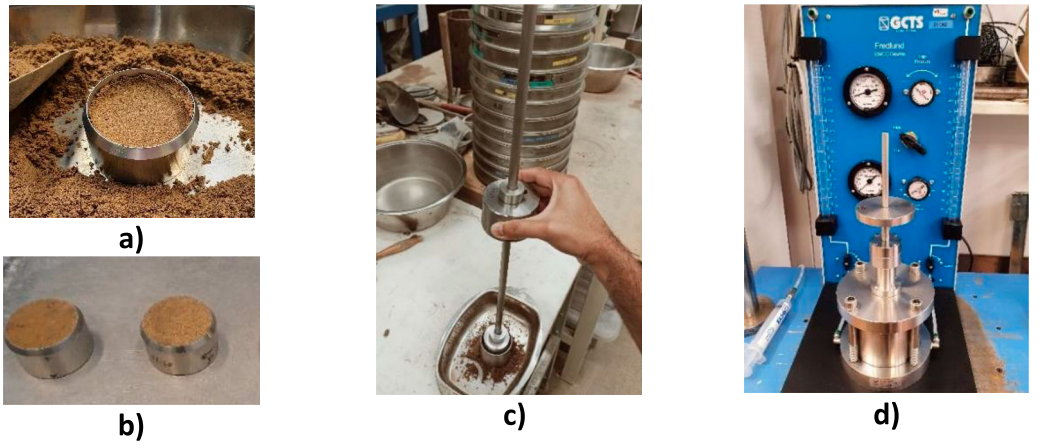

Figure 3. Soil Water Characteristic test (a) sample compaction (b) compacted sample in the final lift (c) prepared samples (d) SWC-150 Pressure plate apparatus.

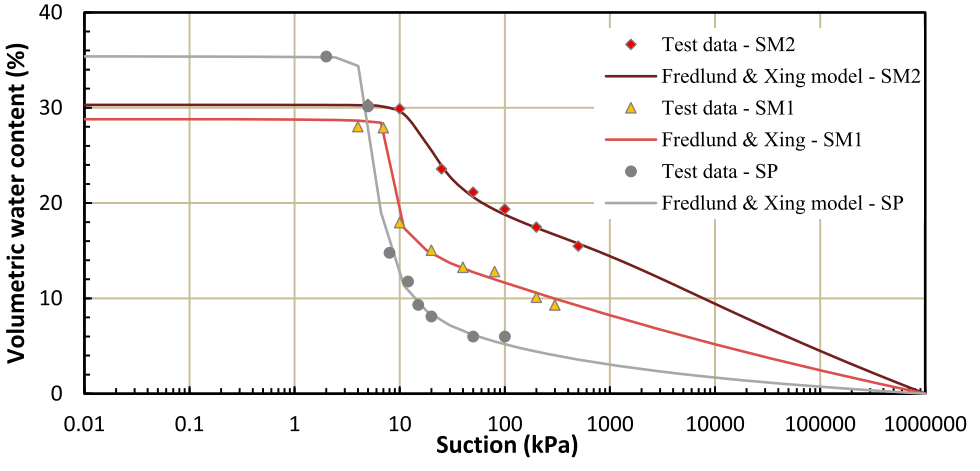

Figure 4. SWRC for the selected materials.

where $C(\psi)$ is a correction factor for the residual suction value (ψ_r); θ_s is the saturated volumetric water content; e is the Euler's constant; a_f is related to the AEV; n_f is the rate of desorption after AEV (Zapata, 2018) related to the pore-size distribution [31]; whereas m_f is related to the residual water content (Zapata, 2018) and represents the model skew (McCartney, 2007).

A soil's AEV marks the frontier between saturated and unsaturated states, while ψ_r determines when the water phase between particle interstices is discontinuous, which makes any reduction in moisture content more difficult by mechanical means.

Figure 4 presents the results of the SWRC tests and the fitting parameters are shown in Table 2. The results show that the material with more fines content SM2 yields more suction in comparison with SM1 and SP at similar moisture levels, as expected.

The soil's SWRC fitting parameters allow inferring the yielded suction at different moisture levels. Such estimation was used when homogenising samples to different post-compaction moisture targets, as will be further detailed in the manuscript.

Table 2. SWRC fitting parameters for the Fredlund & Xing model (1994).

Parameters	Description	unit	SP	SM1	SM2
ψ_r	Residual suction	[kPa]	35	80	750
a_f	Related to AEV	[kPa]	4.98	7.16	12.95
n_f	Related to pore-size distribution	[-]	10.32	36.53	4.51
m_f	Related to desorption rate	[-]	0.52	0.18	0.21
R^2	Coefficient of determination	[-]	0.998	0.996	0.996

Sample preparation for RLT tests

The specimens' dimensions for the M_R tests were 200 mm in height by 100 mm in diameter and were prepared at OMC, targeting 95% of the modified Proctor max dry density. Samples were prepared in a three-split mould and compacted in 9 layers (Figure 5(a)). The corresponding material for each lift was tamped before the blows were applied and the surfaces' layers were scratched before adding material on the subsequent lifts to enhance adhesion between layers.

Thereafter, the samples were allowed to homogenise to pre-determined moisture states before being mounted in the triaxial cell. This was done to ensure moisture equilibrium within the sample but also to accelerate suction equilibrium. For each material, a reference sample at OMC was used to contrast with four other post-compaction moisture states: two above optimum and two dry of optimum. The moisture states were based on the seasonal variation of moisture content for similar materials as measured in the field (Erlingsson & Ullberg, 2017; Saliko & Erlingsson, 2023; Salour & Erlingsson, 2013). Specimen details are found in Table 3.

Two methods were used to increase the moisture content of a specimen: to increase slightly, the steps included involving it with a membrane, enclosing it with a three-split mould to act as a holder, adding water, sealing the membrane temporarily to let the water be soaked in and finally remove the three split mould to assemble the specimen in the triaxial cell (Figure 5(b)). The last image on the right-hand side of Figure 5(b) depicts the sample after having soaked the water. Increasing the moisture closer to full saturation was done after the specimen was mounted in the triaxial cell, where a saturation ramp was imposed into the sample.

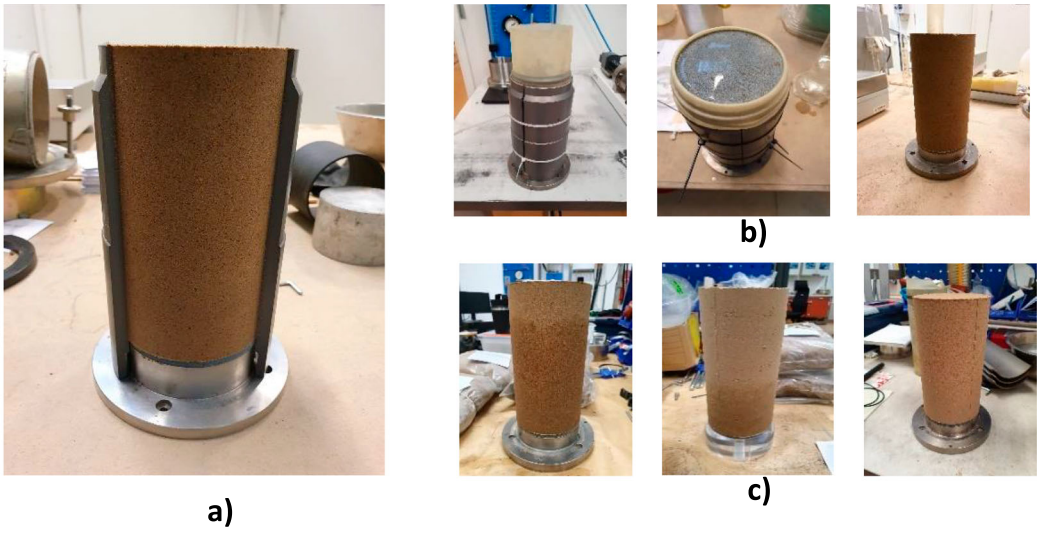

Figure 5. (a) Compacted sample within split mould (b) Increasing the post-compaction moisture content (c) Lowering the moisture content.

Table 3. Sample details for MS-RLT tests of the selected materials at five moisture contents.

Material	Sample ID	Grav. moisture content w [%]	Degree of saturation S_r [%]	Dry density ρ_d [g/cm^3]	Void ratio e [-]	Suction ψ_m [kPa]
SP	SP#1	7.9	42.1	1.75	0.50	8
	SP#2	11.6	63.1			7
	SP#3 (OMC)	15.3	74.6			6
	SP#4	16.1	86.3			3
	SP#5	17.4	93.2			0
SM1	SM1#1	4.9	33.2	1.92	0.38	200
	SM1#2	7.7	53.6			45
	SM1#3 (OMC)	8.7	62.0			10
	SM1#4	9.7	72.5			8
	SM1#5	15.0	95.8			0
SM2	SM2#1	5.7	45.8	2.00	0.32	550
	SM2#2	7.5	58.6			200
	SM2#3 (OMC)	8.9	79.0			100
	SM2#4	10.3	94.7			10
	SM2#5	12.4	97.0			0

Decreasing the degree of saturation was done by letting the sample air-dry until a pre-determined weight loss was achieved, as can be seen in Figure 5(c). The steps followed to lower the moisture included weighting every two hours and involving it with a membrane after achieving the targeted weight loss. From left to right, the Figure 5(c) depicts the gradual loss of water.

The samples have been prepared identically, there is, using the same compaction effort, but small deviations in water content from the reference value (optimum content) occurred during the sample preparation, which coupled with some material heterogeneity, resulted in a slight variation in dry density ρ_d and void ratio e. Nevertheless, such variation did not surpass 5%, which was deemed adequate.

Suction-controlled RLT tests for M_R

In the present study, RLT tests as per AASHTO T:307 was used to characterise the M_R. As this is a quick test, with 100 load applications per stress level, suction-control was adopted to avoid confounding issues that can arise from suction fluctuation during testing, i.e. the tests were conducted with constant moisture content. The suction-controlled RLT tests employed the axis translation technique, which consists of increasing the air and water pressures within the sample so that suction can be established without the water phase going into tension, which under normal atmospheric conditions would result in cavitation (Marinho et al., 2008).

The stress levels, number of load applications, load shape and frequency for the M_R tests were applied as per AASHTO T:307 for subgrade soils (Table 4). After a period for moisture and suction equilibrium, as described in the previous section, which took place over one to two days, depending on the material's permeability, the sample was mounted to the pedestal in the triaxial cell. Thereafter, the axis translation (AT) technique was employed to attain and sustain suction in the sample throughout the RLT test. Figure 6 shows an illustration of the apparatuses for testing unsaturated materials.

Suction attainment consisted of applying a positive u_a via the top cap and a positive u_w via the pedestal, while applying a confining stress σ_3 offset by the u_a, generating a net confining stress $\sigma_{3\text{net}} = \sigma_3 - u_a$. The attainment is complete when the volume change in the air and water pressure controller reaches a standstill (Figure 7). To allow such equilibrium to take place, the pedestal is equipped with a High Air Entry Value (HAEV) ceramic stone, which blocks the throughput seepage of air, up to $u_a = 1500$ kPa, and therefore maintains a pore-pressure gradient $u_a - u_w$ which is equivalent to matric suction, according to the AT technique (Marinho et al., 2008).

After suction attainment, suction control consisted of exerting a constant u_a and u_w to maintain a constant pore-pressure gradient during the dynamic phase of the test. The excess pore-water pressure

Table 4. RLT stress paths for testing subgrade soils as per AASHTO T-307.

Sequence	Net conf. press σ_{3-net} [kPa]	Max deviatoric stress σ_d per stress path[kPa]					# cycles
		1	2	3	4	5	
0 (Conditioning)	41.4	27.6	–	–	–	–	500–1000
1	41.4						
2	27.6	13.8	27.6	41.4	55.2	68.9	100
3	13.8						

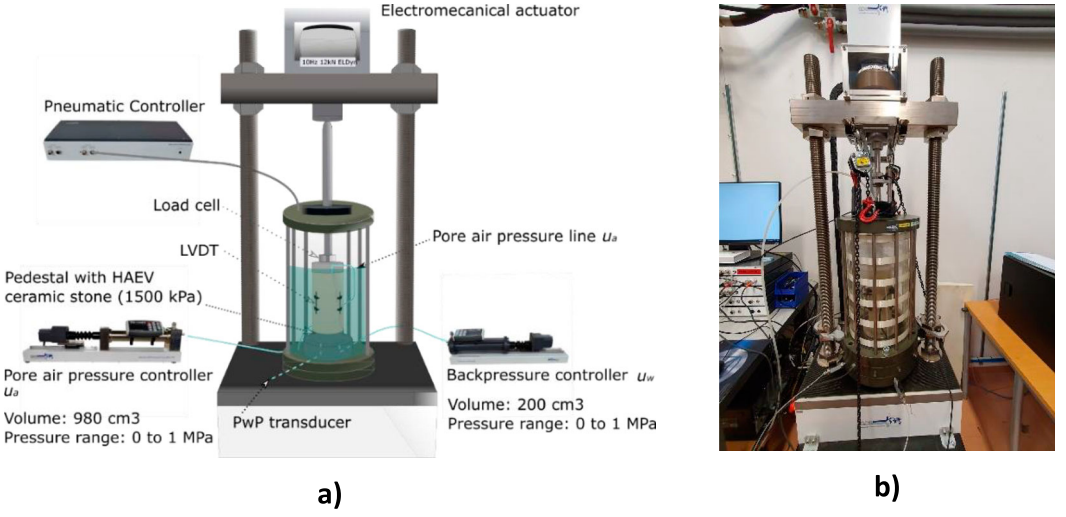

Figure 6. Setup for dynamic testing of unsaturated soils (a) illustration with all apparatuses (b) Triaxial cell with a sample mounted in the ELDyn triaxial testing system (GDS Instruments).

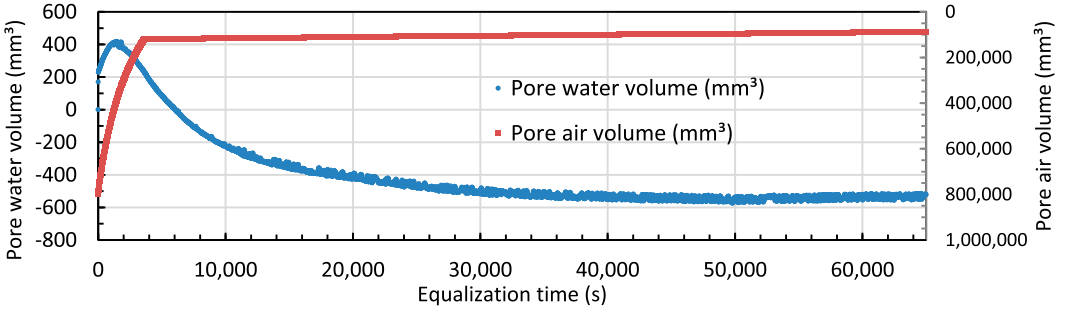

Figure 7. Suction attainment for Sample SM1#2 as per Table 3.

(PwP) generated due to load application was negligible for the unsaturated specimens, and thus the pressure gradient was deemed constant, as can be seen in Figure 8. Indeed the PwP transducer was connected externally to the sample, so in case of PwP fluctuation with load application, this was not captured by the transducer. Similarly, for the air and water pressure controllers, the externally measured pressures did not capture any significant fluctuation during loading.

The dynamic phase of the test (Table 4) consisted of 15 stress paths divided into 3 loading sequences where the confining stress is constant, and a total of 100 load applications were applied per stress path. The applied deviatoric stress σ_d divided by the average resilient strain ε_r for the last

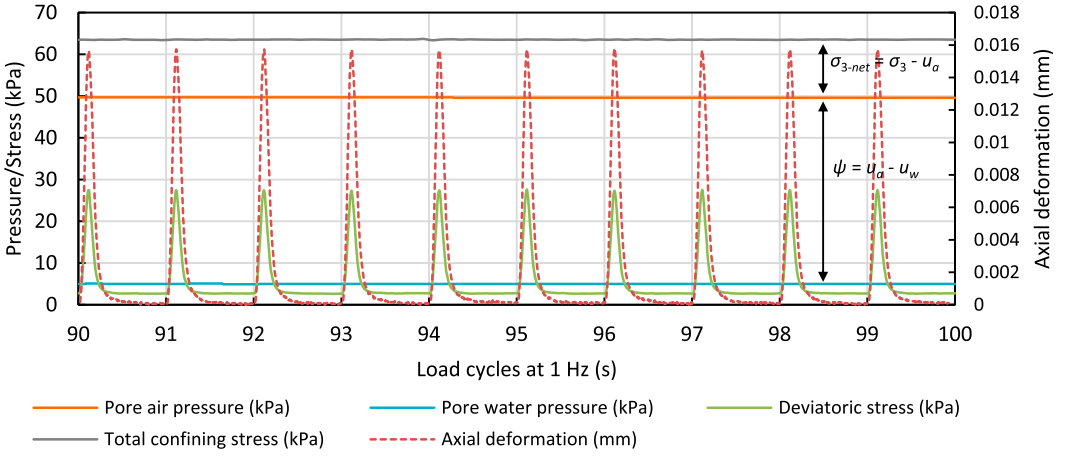

Figure 8. Control and response variables during loading sequence 3, stress path 2 according to Table 4, for Sample SM1#2 as per Table 3. The last 10 cycles in the stress path are shown.

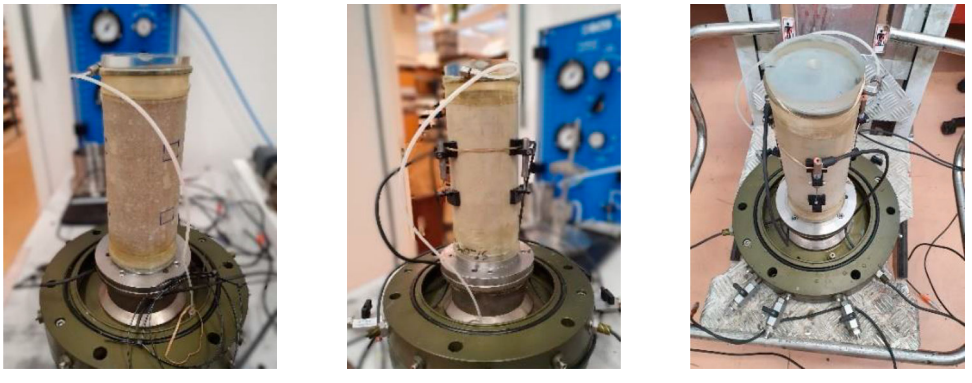

Figure 9. RLT test sample mounting (a) mounted in the triaxial pedestal after moisture homogenisation (b) attachment of LVDTs (c) transport to the load frame.

5 load applications gives the M_R. The dynamic loading consisted of a haversine shape with 0.1s load pulse followed by 0.9s rest period, therefore resulting in a load frequency of 1 Hz. Figure 8 shows the control and response variables of the last 10 cycles of a loading sequence conducted in Sample SM1#2, as per Table 3.

The maximum vertical cyclic load, recorded by the load cell and divided by the sample's area, computes as σ_d while the respective deformation response of each cycle loop (peak and valley measurements) is recorded by three linear variable differential transformers (LVDTs) spaced at 120°. The LVDTs were installed in the third middle of the sample, having a gauge length of 70 mm, as seen in Figure 9, and thus the measured deformation by the gauge length computes as ε_r.

Results and discussion

Test results

An example of the stress–strain relationship of each soil in the RLT test is shown in Figure 10, where 100 data points per load pulse are plotted showing the strain development during the loading and

unloading of each pulse. It shows the average axial strain ε_a of the last 5 load cycles (96–100th load cycles) relative to the nominal ε_a recorded at the beginning of each load cycle, recorded in the same stress path (3rd loading sequence and 3rd stress path, according to Table 3, $\sigma_1 = 41.4$ kPa and $\sigma_3 = 13.8$ kPa) for specimens at different moisture levels, denoting their sensitivity to the latter.

Furthermore, it can be seen that the two coarser materials, SP and SM1, have similar stress strain behaviour, although SM1 is slightly more stable even at higher moisture levels, whereas SM2 shows a stiffer response in dry states and a softer response in wet states. This behaviour is further detailed in the coming subsections.

Figure 11 shows the ε_r against the deviatoric stress obtained for all moisture states as in Table 3 and for the 15 stress paths as in Table 4. Contrasting with Figure 10, where only one stress path was shown, Figure 11 does not show the recorded relative ε_a under cyclic loading but rather the peak relative (recoverable) ε_a associated with each stress level, which is the ε_r.

Such representation allows observing the influence of the confining pressure σ_3 and as a consequence of the bulk stress θ_b; the recorded ε_r is directly proportional to q but inversely proportional to σ_3 and θ_b. Each sample, representing a different moisture content, have its results interval colour-demarcated and the furthest to the right data points under each colour region denote the lowest confining pressure. Figure 11(c) exemplifies this aspect for the sample SM2 close to saturation (SM2#5).

Furthermore, analysing the results of the 5 moisture contents and all stress paths permits verifying the coupled influence that moisture and stress levels have on the resilient behaviour of subgrade soils. For SP and SM1, the influence of moisture is linear while for the more fine-grained SM2, it is linear at dry states but becomes non-linear at moisture states above optimum. In addition, SM2 is more sensitive to higher moisture levels than the other two materials with less fines.

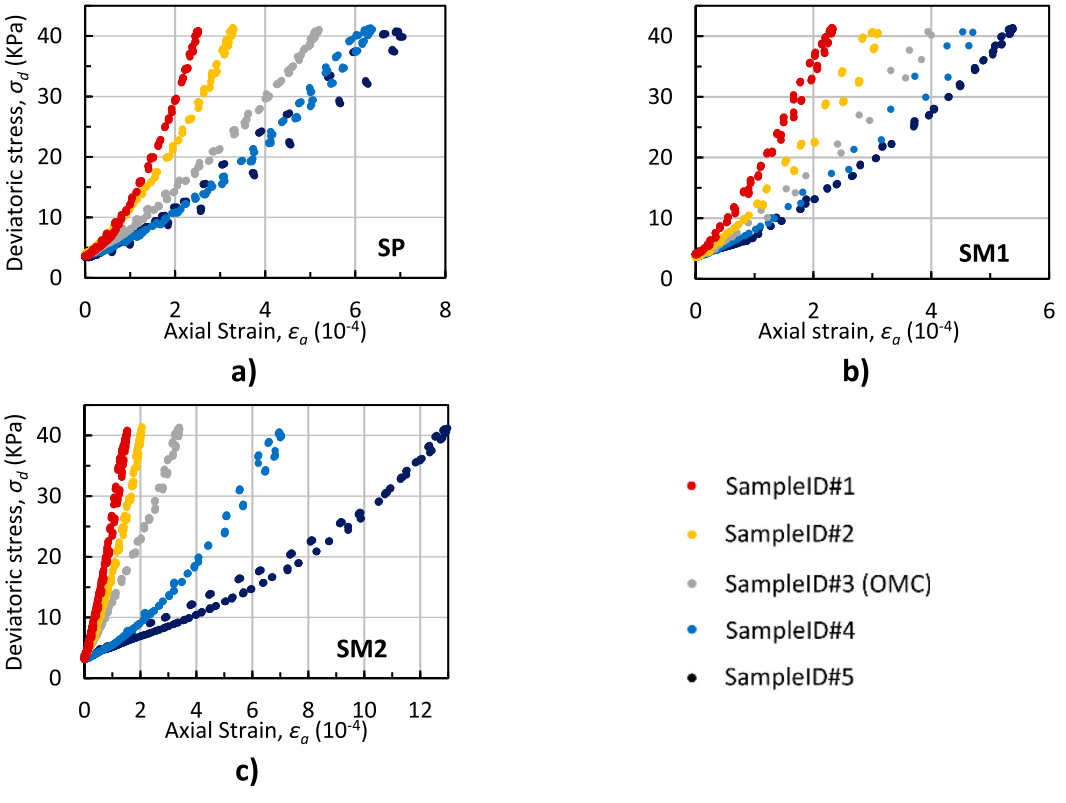

Figure 10. Stress – strain relationships for loading sequence 3 and stress path 3 ($\sigma_3 = 13.8$ kPa, $\sigma_d/\sigma_3 = 3$) at 5 different moisture contents as shown in Table 3 (a) SP bSM1 and (c) SM2.

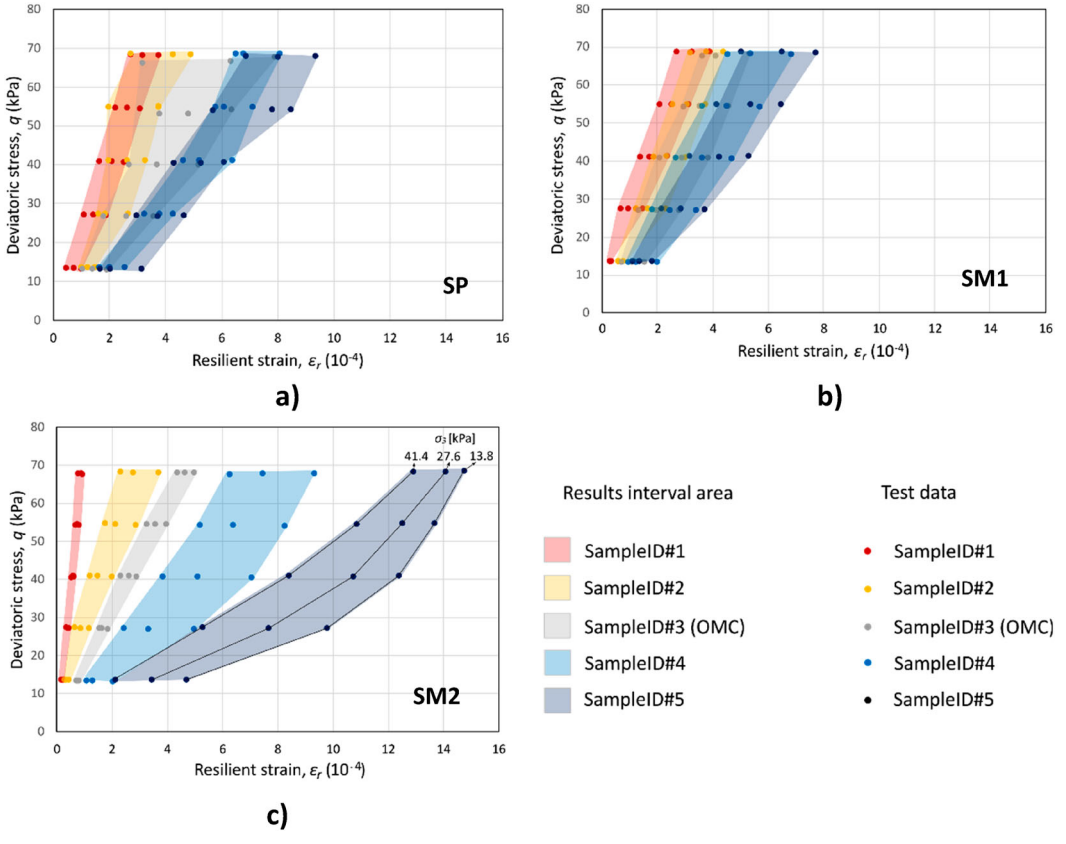

Figure 11. Stress – resilient strain relationships for all stress paths, at 5 different moisture contents as shown in Table 3 (a) SP (b) SM1 and (c) SM2.

When it comes to the influence of suction, Figure 12(a) shows a non-linear relationship between the measured ε_r and ψ. For SP and SM1, the relationship is roughly linear in suction levels lower than the yield at OMC and non-linear when suction is higher than the suction yield at OMC. Whereas for SM2, it is non-linear at any suction level, although the slope is flatter at higher than OMC suction levels. The non-linearity of χ (Equation 4) becomes evident in Figure 12(b). Furthermore, the contribution of suction stress to the effective stress (Equation 3) is more substantial for SM2, of lesser contribution for SM1 and even lesser for SP.

Stress based models

Cary & Zapata's model (Equation 7), a stress-based model that considers suction as an independent variable, was selected here for further analysis of the observed data as it was verified for materials with similar properties in Sweden (Salour et al., 2015). In addition, another stress-based model was trialled – aiming to better fit M_R on the wet side – where a revision of the Liang et al. (2008) model (Equation 8) is proposed.

As can be seen in Figure 8, the PwP transducer did not register a change in pore-water pressure during the RLT test, and as suction was kept constant throughout the tests, Equation 7 (Cary & Zapata's model) was simplified into Equation 14. The constant PwP might be due to the small magnitude of the dynamic loads coupled with the resting period between load pulses.

The revision of the Liang et al. (2008) model, presented in Equation 15, entails changing the stress component described by the model parameter k_2 from bulk stress θ_b to net mean stress

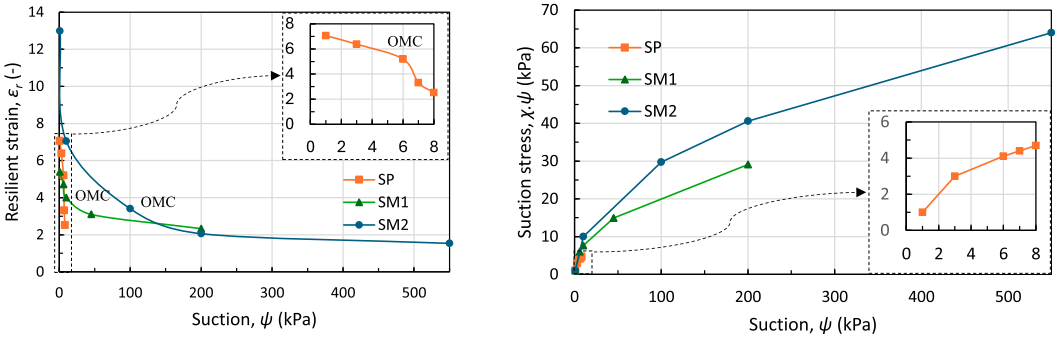

Figure 12. Measured resilient strain against suction and suction stress variables at loading sequence 3 and stress path 3 as in Table 3 ($\sigma_3 = 13.8$ kPa, $\sigma_d/\sigma_3 = 3$) (a) SP (b) SM1 (c) SM2.

$\sigma' = p_{net} = (\sigma_1 + 2\sigma_3)/3 - u_a$, to better conform with the physical concept of the Bishop's effective stress (Equation 3), which adds suction stress to the net mean stress. Therefore, both models and consequently charts used in this analysis are given in terms of net stress.

Moreover, for the calculation of the Bishop's parameter χ, the approach proposed by Khalili and Khabbaz (1998) was adopted because it was conceived based on experimental data of shear strength tests conducted under suction control in a similar range to this study, i.e. 0–500 kPa, showing a unique relationship between χ and the suction ratio (Equation 4) with good correlations ($R^2 > 0.98$) for 13 naturally occurring soils including sandy soils.

$$M_R = k_1 p_a \left(\frac{\theta_{b-net}}{p_a}\right)^{k_2} \left(\frac{\tau_{oct}}{p_a} + 1\right)^{k_3} \left(\frac{\psi_0}{p_a}\right)^{k4} \tag{14}$$

$$M_R = k_1 p_a \left(\frac{p_{net} + \chi \cdot \psi_m}{p_a}\right)^{k_2} \left(\frac{\tau_{oct}}{p_a} + 1\right)^{k_3} \tag{15}$$

Figure 13(a, c and e) presents the M_R measurements and the model fit by Equation 14 (Cary & Zapata model); the results are presented in $\tau_{oct} - \psi - M_R$ space. Figure 13(b, d and f) presents the M_R measurements and the model fit by Equation 15 (modified Liang et. al model); the results are presented in $\tau_{oct} - p' - M_R$ space. The complete dataset for each soil type containing 75 entries, i.e. 5 moisture content and 15 stress paths according to AASHTO T-307, was used for obtaining a best fit and generating the predicted values (shown as surfaces in Figure 13). Measured values are shown for $\sigma_{3-net} = 14$ kPa for practical purposes, given this constraint level is expected in the upper part of the subgrade level (Everton & Erlingsson, 2025).

Curve fitting

The least squares method was employed to fit the test data to the predictive models and Table 5 presents the results. For the stress-based model (Figure 13(a, c and e)), it can be noted that the poorly graded sand SP shows stress hardening whereas SM1 shows stress hardening only at lower suction values and leans towards a neutral behaviour to shear at higher suction values; similar properties apply for SM2, but it can be noted that it leans towards stress softening with increasing τ_{oct}.

In fact, the behaviour of the SP material is typical of granular materials that stiffen with increased stress levels (Lekarp et al., 2000). The resilient behaviour of the material with higher fines content, SM2, is similar to the study conducted on a silty material that suggests that the influence of the deviatoric stress is more substantial at higher suction (Ng et al., 2013). The material with medium fines content, SM1, behaves more like sand at lower suction levels and more like the material SM2 at higher suction levels.

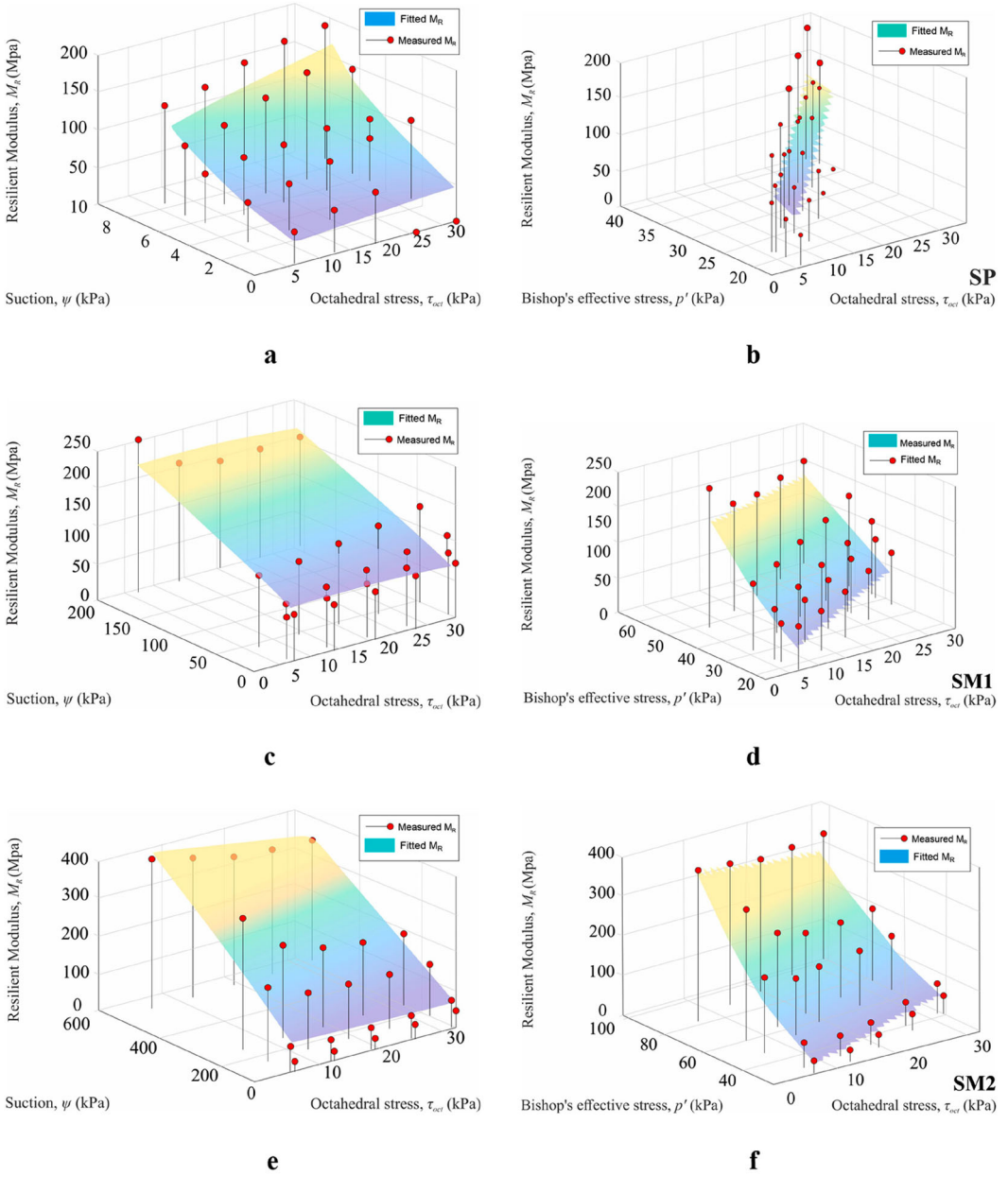

Figure 13. Cary and Zapata model for (a) SP, (c) SM1 and (e) SM2; Modified Liang et al model for (b) SP (d) SM1 and (f) SM2.

For the modified Liang et al. model (Figure 13(b, d and f)), it can be noted that the model better fitted the M_R on the wet side of optimum for the two silty sands SM1 and SM2, while overall providing a good fit for those materials, similarly to that obtained using the Cary & Zapata model. As the model was originally aimed to fit cohesive materials (Liang et al., 2008), this might explain the poor fit for the poorly graded sand SP. Hence, this result suggests that the stress-based model wherein suction changes the effective stress might only be suitable for materials with a considerable finer fraction. In other words, obtaining a unique set of parameters k_1, k_2, and k_3 regardless of the moisture state is not

Table 5. Regression parameters for the selected stress-based and moisture-based models.

Model	parameter	unit	SP	SM1	SM2
Cary & Zapata model (Equations 7 and 14)	k_1	(-)	500	1638	1330
	k_2	(-)	0.694	0.797	0.590
	k_3	(-)	−0.338	−2.724	−2.668
	k_4	(-)	16.052	0.762	0.842
	R^2	(-)	0.834	0.837	0.902
Modified Liang et al. (Equation 15)	k_1	(-)	2650	7293	6754
	k_2	(-)	0.837	1.572	2.105
	k_3	(-)	−0.202	−3.126	−3.403
	R^2	(-)	0.264	0.813	0.896

achievable using Equation 15 (modified Liang et. al model) for subgrades with different gradations, as it was possible to do when using Equation 14 (Cary & Zapata model).

Using the models presented in Figure 13, the correlations for measured and predicted M_R are presented in Figure 14. As anticipated, the Cary & Zapata model fitted the data quite well, with a coefficient of determination $R^2 > 0.83$ in all cases. However, a closer examination of the Cary & Zapata model predictions shows that the model overpredicts the M_R on the wet side for some of the materials, namely the silty sand with higher fines content (SM2) and for SM1 at lower stress levels, suggesting a cautionary approach must be adopted when using the model to design pavements subject to seasonal moisture variation. On the other hand, the modified Liang et al. model fixed this issue observed for the silty sands, for which the results show quite good agreement with a coefficient of determination $R^2 > 0.81$. As already pinpointed, the modified Liang et al model has shown poor agreement with the experimental data for the poorly graded sand (SP) and Figure 14(d) just emphasises this observation.

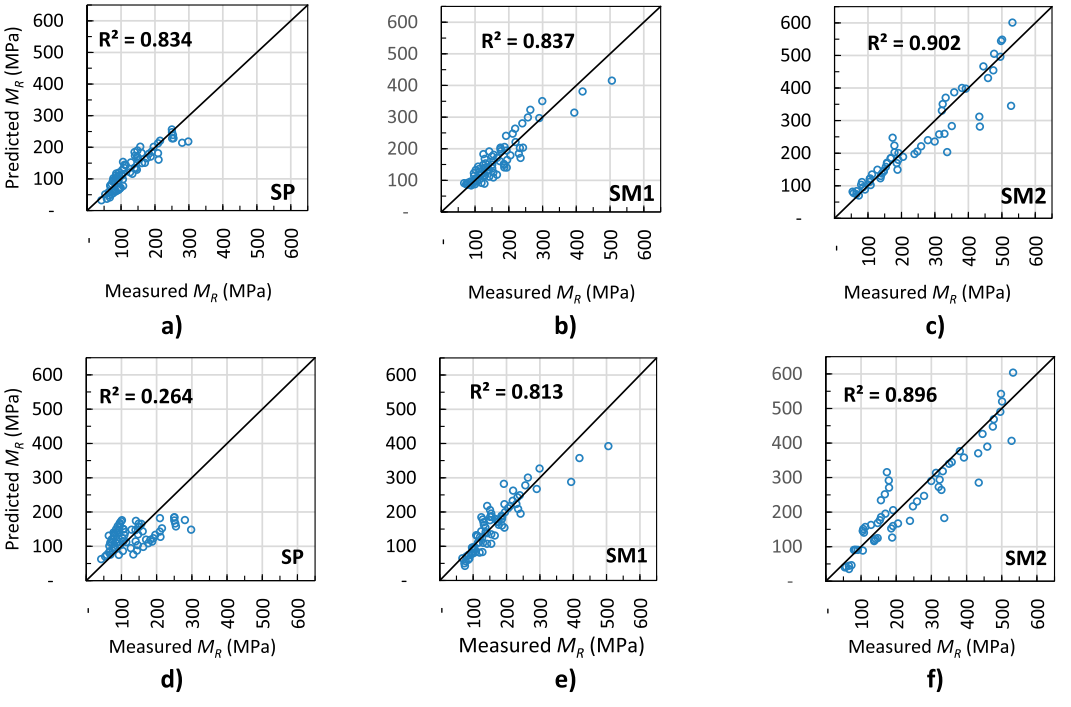

Figure 14. Goodness of fit for the Cary & Zapata model (a) SP (b) SM1 (c) SM2; modified Liang et al. (2008) model (d) SP, (e) SM1, (f) SM2.

Table 6. Regression parameters for the modified stress-based and suction-based models.

Model	parameter	unit	SP	SM1	SM2
MEPDG model (Equation 11)	a	(-)	−0.324	−0.270	−0.568
	b	(-)	0.326	0.269	0.435
	k_m	(-)	7.864	6.970	5.963
	R^2	(-)	0.983	0.966	0.876
Suction-based model (Equation 17)	$M_{R\text{sat}}$	(MPa)	64.1	77.9	33.1
	α_1	(-)	0.0074	38.8247	17.6810
	β_1	(-)	4.632	0.278	0.574
	Ψ_{opt}	(kPa)	6	10	100
	R^2	(-)	0.976	0.950	0.998

Moisture-suction models

In this section, the MEPDG moisture-based model, one of the most commonly adopted in pavement design, is evaluated and compared with a simple suction-based model, which is proposed based on the stress-based model given in Equation 8 (Khoury et al., 2009), drawing on the experimental data extracted from both the RLT and SWRC tests conducted in this study. Considering ψ_m equals 0 in saturated conditions, Equation 8 is transformed into Equation 16, and therefore, the M_R at any given moisture/suction condition is given by adding $\alpha_1 {\psi_m}^{\beta_1}$ to $M_{R\text{sat}}$, which denotes the stiffness under a nearly fully saturated condition. Equation 17 presents the suction-based model, where the ratio of M_R is a function of $M_{R\text{sat}}$, ψ_m, ψ_{opt} and the latter represents the matric suction at optimum conditions as indicated in Table 3.

$$M_{R\text{sat}} = k_1 p_a \left(\frac{\theta_b}{p_a}\right)^{k_2} \left(\frac{\tau_{\text{oct}}}{p_a} + k_4\right)^{k_3} \tag{16}$$

$$\frac{M_R}{M_{R\text{opt}}} = \frac{M_{R\text{sat}} + \alpha_1 {\psi_m}^{\beta_1}}{M_{R\text{sat}} + \alpha_1 {\psi_{\text{opt}}}^{\beta_1}} \tag{17}$$

Figure 15(a, c and e) shows the M_R measurements at $\sigma_{3-\text{net}} = 14$ kPa and $\sigma_d = 41$ kPa, and the model fit by Equation 11 (MEPDG moisture-based model); the results are shown as the ratio of $M_R = f[(S\text{-}S_{\text{opt}})]$. Figure 15(b, d and f) shows the M_R measurements at $\sigma_{3-\text{net}} = 14$ kPa and $\sigma_d = 41$ kPa, and the model fit by Equation 17 (proposed suction-model); the results are shown as the ratio of $M_R = f[\psi_m]$. Similarly to the fitting approach performed for the stress-based models, all data points for each soil type were used for obtaining best fit parameters and plotting the best-fit line. The choice of representing the stress state $\sigma_{3-\text{net}} = 14$ kPa and $\sigma_d = 41$ kPa in Figure 15 was done for practical purposes, as recommended by the National Cooperative Highway Research Program (NCHRP) 1-28A (NCHRP, 2003).

For the moisture-based model (Figure 15(a, c and e)) suggested values for the material parameters given according to their particle size distribution were used to plot the predictive curves referred to as MEPDG in the charts.

Curve fitting

The same method as described in the previous section was employed to fit the test data to the predictive models and Table 6 presents the material parameters. For the MEPDG moisture-based model, the modelling conducted in this study considered the logarithm of the average ratio of M_R for all stress paths on the wet side ($M_{R\text{wet}}/M_{R\text{opt}}$) and dry side ($M_{R\text{dry}}/M_{R\text{opt}}$). This approach was better suited to fit the data than the minimum ratio on the wet side and maximum ratio on the dry side, for a and b respectively, as suggested in the MEPDG manual (ARA, 2004) and resulted in excellent fit with $R^2 > 0.9$ for SP and SM1 and a very good fit for SM2 ($R^2 = 0.88$). $M_{R\text{wet}}$ accounts for the resilient modulus obtained in the condition closer to saturation (SampleID#5 in Table 3), while $M_{R\text{dry}}$ is the resilient modulus obtained for the dryer samples (SampleID#5 in Table 3)

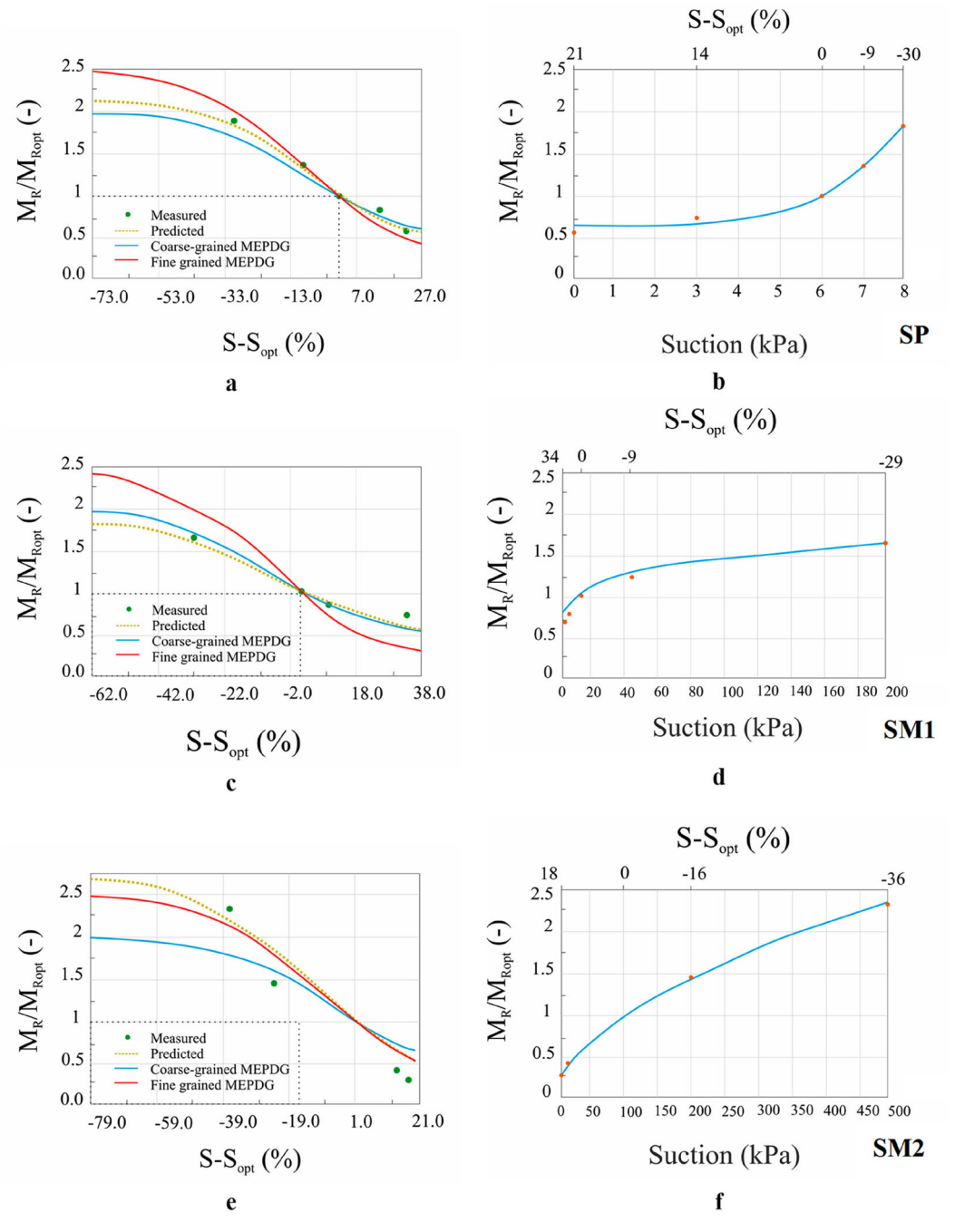

Figure 15. MEPDG moisture-base model for (a) SP, (c) SM1 and (e) SM2 (e); Suction-based model for (b) SP (d) SM1 and (f) SM2.

For SP and SM1, the fitted parameters are not distant from the parameters suggested in the MEPDG for coarse-grained materials; for SM2, although the fitted parameter indicative of the wet side *a* is quite close to the MEPDG for fine-grained materials, the parameter indicative of the dry side *b* is slightly higher, suggesting that the ratio of M_R limited at 2.5 is conservative at higher suction values (lower moisture content) for fine-grained materials.

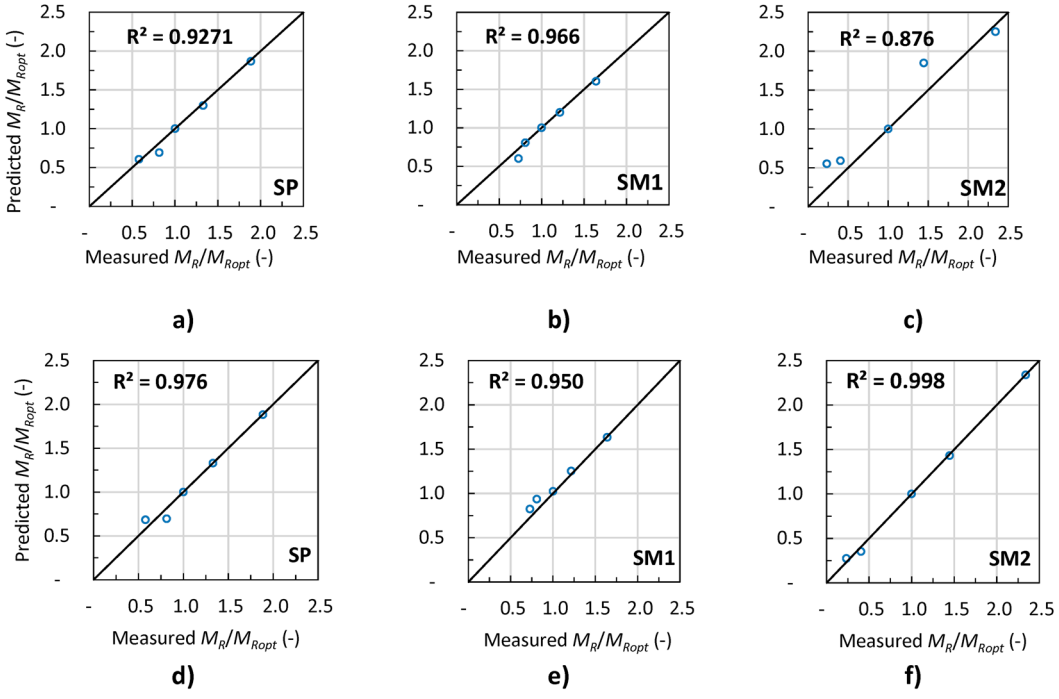

Figure 16. Goodness of fit for the MEPDG model (a) SP (b) SM1 (c) SM2; Suction-based model (d) SP, (e) SM1, (f) SM2.

For the suction-based model (Figure 15(b, d and f)), an excellent fit was obtained ($R^2 > 0.95$). Furthermore, it can be noted that the maximum ratio of M_R on the dry side is similar to the one suggested in the MEPDG model, with the difference that the scale here is adjusted to what is expected to be the maximum suction yielded by each material when it is in a dry state in the field. Hence, even though finer-grained materials might develop higher suction and consequentially higher M_R, such conditions might only be attainable in the laboratory.

As can be seen in Figure 15(b, d and f) and further down in Table 6, the shape and material parameters of the silty sands SM1 and SM2 have some resemblance, which denotes a similar pattern of non-linearity to the induced stress. On the other hand, the shape and material parameters obtained for the granular material SP go in a different direction and denote a different non-linearity. In fact, re-examining Figure 13(a, c and e), the difference in non-linearity becomes evident, where SP is characterised by its stress-hardening, SM2 leans more towards stress-softening, and SM1 behaves like the SP at lower suction levels but more like SM2 at higher suction levels.

A correlation between measured and predicted M_R is shown in Figure 16, Whereas the suction model showed excellent agreement ($R^2 > 0.9$) for all tested materials.

Discussion

Suction-controlled RLT tests conducted at 5 different moisture-suction levels showed that ε_r increases at higher moisture/lower matric suction levels, with the more densely packed material and with high fines (39%), SM2, showing the lowest and highest ε_r in dry and wet states, respectively, from the three tested soils. The second more densely packed and with less fines (17%), SM1, was the most stable, not showing as big a difference in the various moisture-suction levels tested. The least densely packed and with less fines (4%), SP, was not as stable as SM1, but more stable than SM2, although it performed worser than the latter at optimum and dryer states.

The analysis of the coupled effect of moisture and stress levels (Figure 11) suggested that the effect of moisture may not be considered proportional regardless of the stress level for the materials with high fines content, such as SM2, which is the hypothesis used when employing the MEPDG M_R-moisture model (Equation 11), and thus stress-suction models are favoured in this case.

Analysing the effect of suction, a non-linear behaviour was observed for all tested materials, although the results for the coarser-grained materials SP and SM1 showed a roughly linear relationship at moisture states below OMC, as can be seen in Figure 12. Furthermore, the calculated suction stress appeared to be highly related to the material's SWRC properties (AEV and shape of the curve) and consequently to the fines content.

Results were fitted with two stress-based models for predicting the M_R, each with a different interpretation of the contribution of suction. The model that incorporates suction to the effective stress (Equation 15) produced better fits for the silty sands but a poorer fit to SP, compared to the model that adds suction as an independent variable (Equation 7/14), corroborating the analysis of the relationship between suction stress and suction presented presented in section 5.1, Figure 12.

Ideally, a unique set of material parameters for the prediction models is preferred and in that sense Cary & Zapata model (Equation 7/14) can deliver on that aspect for all tested materials, but attention needs to be taken not to overpredict M_R on the wet side, as the results suggested that model was prone to that for some materials and at low-stress levels, which was not observed in the modified Liang et al. model (Equation 15).

The evaluation of stress-suction models fulfils the aim of this study, which was to improve M_R prediction models for sandy subgrades by proposing a modification to the Liang et al. model based on Bishop's effective stress principle. However, as it was noted, the model was not suitable for a poorly graded material with low fines content. Therefore, the motivation for not capturing the resilient behaviour of soil such as SP is examined. The implication of such a finding may be that this concept of effective stress does not explain the resilient behaviour of granular materials with low fines content, such as soils employed as sub-base and base.

As suggested by Park et al. (2024), suction stress can be divided as a sum of two stresses: meniscus stress and bulk water stress. In this postulation of suction stress, bulk water stress reduces suction stress while meniscus stress increases it. Considering SP has low fines content and is poorly distributed it has large pore interstices; hence the water meniscus tends to have large radii even in drier states, and therefore, low meniscus stress. Moreover, as noted by Azizi et al. (2023), Bishop's effective stress neglects the normal forces acting on soil particles due to water menisci because it considers the effect of suction on the average skeleton stress. Due to this, they propose a suction bonding parameter ξ that contributes to M_R independently from the soil's stress-state. These two hypotheses offer plausible explanations for the poor fit obtained for SP using the model based solely on the Bishop's effective stress.

Furthermore, a moisture-based model was trialled, where the MEPDG M_R-moisture model (Equation 11) with fitted parameters predicted the results reasonably well, but it was noted that the MEPDG suggested parameters for fine-grained materials underpredicted the M_R for SM2 at lower moisture levels, when suction is higher, while slightly overpredicting it at higher degrees of saturation. Thus, employing a different modelling strategy to obtain the fitted parameters rather than using the literature values proved to be successful as R^2 was higher than 0.9. The approach consisted of adopting the average logarithm of the ratio of M_R on the wet and dry sides, instead of the minimum and maximum logarithm respectively. That requires, as a minimum, a control sample at OMC, as well as one on the dry side and another on the wet side.

In addition, a suction-based model was proposed (Equation 17), where the M_R results in a near saturation condition are used as baseline to which a suction component is added. The fits obtained with that model matched the quality of the fit obtained using the MEPDG M_R-moisture model; however, by setting the baseline at the near saturation condition instead of the optimum, a better fit was obtained for the material with more fines content, which is also the weakest in the saturated condition.

Conclusion

This study modelled the resilient behaviour of sandy soils, where M_R prediction models were evaluated and showed the effect of stress levels coupled with moisture/suction on subgrade soils, comprising one poorly graded sand SP and two silty sands SM1 and SM2. The results demonstrate that there is a clear influence of suction in their stiffness behaviour, and that the magnitude of such contribution is highly dependent on the finer fraction. In addition, the unsaturated soil properties obtained in the SWRC were substantial to customise the suction-controlled RLT tests and to analyse the results, by employing soil parameters such as AEV and residual degree of saturation on an M_R prediction model.

In that regard, stress-suction based models and a suction-based model offered a good fit to the experimental data, which is an indicator that they can be used in M-E pavement design considering climate conditions. The main conclusions are as follows:

- Stress and moisture effects: This study confirmed that suction/lower moisture increases resilient modulus (M_R) for all tested sands. The effect of deviatoric stress varied, with hardening behaviour for the poorly graded sand SP, neutral/softening for the silty sand with 39% fines, SM2, and a somewhat mixed behaviour for the silty sand with 17% fines, SM1.
- Modelling M_R: Two stress-based models were evaluated. The Cary & Zapata model offered a single parameter set and a very good fit overall, but overpredicted M_R at high moisture content for the silty sands. The modified Liang et al. model provided better fits for the silty sands, SM1 and SM2, but was not suitable for the poorly graded sand SP, possibly because the low suction yielded in such open-graded material do not contribute much to the average skeleton stress for enhancing the resilient modulus of soils, such as it was observed on the well-graded silty sands with considerable finer fraction.
- Simplified modelling strategies: Two non-stress-based models were evaluated. The MEPDG M_R-moisture model with fitted parameters performed well, but struggled with the finer-grained silty sand, SM2, overpredicting M_R in the wet state and underpredicting it in the dry state. A newly proposed suction-based model performed similarly to the MEPDG M_R-moisture model with the advantage of providing a better fit for SM2.

To conclude, this investigation promoted a better understanding of the resilient behaviour of materials that can be typically found in Southern Sweden and can be used as a reference for similar soils found elsewhere. The study identified the most suitable models according to the material, offering more accuracy to predict M_R at different moisture-suction levels, which is a considerable resource to understand the state of our pavement assets under varying climate conditions. The conclusions of this study are limited to three materials and a further limitation lie in the fact that softening processes were not investigated. Future studies will also investigate whether suction bonding effect can improve the accuracy of $\underline{M_R}$ prediction models for soils.

Disclosure statement

No potential conflict of interest was reported by the authors.

Funding

This research is funded by the Swedish Transport Administration (Trafikverket).

Author contribution

The authors confirm contributions to the paper as follows: problem concept and experimental design: J.H.C. Everton, S. Erlingsson, laboratory tests: J.H.C. Everton, analysis and interpretation of results: J.H.C. Everton, S. Erlingsson, draft manuscript preparation: J.H.C. Everton, manuscript review: S. Erlingsson. All authors reviewed the results and approved the final version of the manuscript.

References

Andrei, D. (2003). *Development of a predictive model for the resilient modulus of unbound materials* [Doctoral dissertation]. Arizona State University.

ARA, Inc., ERES Division. (2004). *Guide for mechanistic-empirical design of new and rehabilitated pavement structures, NCHRP 1-37A Final Report*.

Azizi, A., Kumar, A., & Toll, D. G. (2023). Coupling cyclic and water retention response of a clayey sand subjected to traffic and environmental cycles. *Géotechnique*, *73*(5), 401–417. https://doi.org/10.1680/jgeot.21.00063

Bishop, A. (1959). The principle of effective stress. *Teknisk Ukeblad*, *106*(39), 859–863.

Blackmore, L., Clayton, C. R. I., Powrie, W., Priest, J. A., & Otter, L. (2020). Saturation and its effect on the resilient modulus of a pavement formation material. *Géotechnique*, *70*(4), 292–302. https://doi.org/10.1680/jgeot.18.P.053

Cary, C. E., & Zapata, C. E. (2011). Resilient modulus for unsaturated unbound materials. *Road Materials and Pavement Design*, *12*(3), 615–638. https://doi.org/10.1080/14680629.2011.9695263

Doré, G., & Zubeck, H. K. (2009). *Cold regions pavement engineering* (1st ed.). McGraw-Hill.

Erlingsson, S. (2012). Rutting development in a flexible pavement structure. *Road Materials and Pavement Design*, *13*(2), 218–234. https://doi.org/10.1080/14680629.2012.682383

Erlingsson, S., & Ullberg, J. (2017). Responses and performance of flexible pavements in cold climate due to heavy vehicle loading. In A. Loizos, I. L. Al-Qadi, & T. Scarpas (Eds.), *Bearing capacity of roads, railways and airfields: Proceedings of the 10th International Conference on the Bearing Capacity of Roads, Railways and Airfields (BCRRA 2017)* (pp. 451–457). CRC Press.

Everton, J. H. C., & Erlingsson, S. (2025). Characterising the permanent deformation of subgrade soils under seasonal variation. *Canadian Journal of Civil Engineering*, *52*(*3*), 317–333. http://dx.doi.org/10.1139/cjce-2024-0077

Everton, J. H. C., Saliko, D., & Erlingsson, S. (2022). Freeze-thaw influence on the water retention capacity of silty sand subgrades. In I. Hoff, R. Saba, & H. Mork (Eds.), *Eleventh International Conference on the Bearing Capacity of Roads, Railways and Airfields (BCRRA), Volume 2* (pp. 122–131). CRC Press. https://doi.org/10.1201/9781003222897-10

Fredlund, D. G., & Morgenstern, N. R. (1977). Stress state variables for unsaturated soils. *Journal of the Geotechnical Engineering Division*, *103*(5), 447–466. https://doi.org/10.1061/AJGEB6.0000423

Fredlund, D. G., Morgenstern, N. R., & Widger, R. A. (1978). The shear strength of unsaturated soils. *Canadian Geotechnical Journal*, *15*(3), 313–321. https://doi.org/10.1139/t78-029

Fredlund, D. G., & Xing, A. (1994). Equations for the soil-water characteristic curve. *Canadian Geotechnical Journal*, *31*(4), 521–532. https://doi.org/10.1139/t94-061

Han, Z., & Vanapalli, S. K. (2015). Model for predicting resilient modulus of unsaturated subgrade soil using soil-water characteristic curve. *Canadian Geotechnical Journal*, *52*(10), 1605–1619. https://doi.org/10.1139/cgj-2014-0339

Han, Z., & Vanapalli, S. K. (2016). State-of-the-art: Prediction of resilient modulus of unsaturated subgrade soils. *International Journal of Geomechanics*, *16*(4), 04015104. https://doi.org/10.1061/(ASCE)GM.1943-5622.0000631

Huang, Y. H. (2004). *Pavement analysis and design* (2nd ed.). Pearson/Prentice Hall.

Khalili, N., & Khabbaz, M. H. (1998). A unique relationship for χ for the determination of the shear strength of unsaturated soils. *Géotechnique*, *48*(5), 681–687. https://doi.org/10.1680/geot.1998.48.5.681

Khoury, N., Brooks, R., & Khoury, C. (2009). Environmental influences on the engineering behavior of unsaturated undisturbed subgrade soils: Effect of soil suctions on resilient modulus. *International Journal of Geotechnical Engineering*, *3*(2), 303–311. https://doi.org/10.3328/IJGE.2009.03.02.303-311

Lekarp, F., Isacsson, U., & Dawson, A. (2000). State of the art. I: Resilient response of unbound aggregates. *Journal of Transportation Engineering*, *126*(1), 66–75. https://doi.org/10.1061/(ASCE)0733-947X(2000)126:1(66)

Liang, R. Y., Rabab'ah, S., & Khasawneh, M. (2008). Predicting moisture-dependent resilient modulus of cohesive soils using soil suction concept. *Journal of Transportation Engineering*, *134*(1), 34–40. https://doi.org/10.1061/(ASCE)0733-947X(2008)134:1(34)

Lu, N., Godt, J. W., & Wu, D. T. (2010). A closed-form equation for effective stress in unsaturated soil. *Water Resources Research*, *46*(5), 2009WR008646. https://doi.org/10.1029/2009WR008646

Lu, N., & Likos, W. J. (2006). Suction stress characteristic curve for unsaturated soil. *Journal of Geotechnical and Geoenvironmental Engineering*, *132*(2), 131–142. https://doi.org/10.1061/(ASCE)1090-0241(2006)132:2(131)

Marinho, F. A. M., Take, W. A., & Tarantino, A. (2008). Measurement of matric suction using tensiometric and axis translation techniques. *Geotechnical and Geological Engineering*, *26*(6), 615–631. https://doi.org/10.1007/s10706-008-9201-8

McCartney, J. S. (2007). *Determination of the hydraulic characteristics of unsaturated soils using a centrifuge permeameter* [PhD thesis]. The University of Texas at Austin. http://citeseerx.ist.psu.edu/viewdoc/download?doi = 10.1.1.822.6593&rep = rep1&type = pdf

NCHRP. (2003). *Harmonized test methods for laboratory determination of resilient modulus for flexible pavement design.* (1-28A).

Ng, C. W. W., Zhou, C., Yuan, Q., & Xu, J. (2013). Resilient modulus of unsaturated subgrade soil: Experimental and theoretical investigations. *Canadian Geotechnical Journal*, *50*(2), 223–232. https://doi.org/10.1139/cgj-2012-0052

Park, H.-S., Kim, B.-S., Kato, S., & Park, S.-W. (2024). Suction stress effects on stress-dependent resilient modulus of subgrade soils. *Road Materials and Pavement Design*, *25*(6), 1229–1248. https://doi.org/10.1080/14680629.2023.2266047

Rasul, J. M., Ghataora, G. S., & Burrow, M. P. N. (2018). The effect of wetting and drying on the performance of stabilized subgrade soils. *Transportation Geotechnics*, *14*, 1–7. https://doi.org/10.1016/j.trgeo.2017.09.002

Rojas, E. (2008). Equivalent stress equation for unsaturated soils. I: Equivalent stress. *International Journal of Geomechanics*, *8*(5), 285–290.

Saliko, D., & Erlingsson, S. (2023). Evaluation of the structural response of two in-service thin flexible pavements under heavy vehicle loading during different seasons by built-in sensors. *International Journal of Pavement Engineering*, *24*(2), 1–18. https://doi.org/10.1080/10298436.2022.2138875

Salour, F., & Erlingsson, S. (2013). Moisture-sensitive and stress-dependent behavior of unbound pavement materials from in situ falling weight deflectometer tests. *Transportation Research Record: Journal of the Transportation Research Board*, *2335*(1), 121–129. https://doi.org/10.3141/2335-13

Salour, F., & Erlingsson, S. (2015). Resilient modulus modelling of unsaturated subgrade soils: Laboratory investigation of silty sand subgrade. *Road Materials and Pavement Design*, *16*(3), 553–568. https://doi.org/10.1080/14680629.2015.1021107

Salour, F., Erlingsson, S., & Zapata, C. E. (2015). Model for seasonal variation of resilient modulus in silty sand subgrade soil: Evaluation with falling weight deflectometer. *Transportation Research Record: Journal of the Transportation Research Board*, *2510*(1), 65–73. https://doi.org/10.3141/2510-08

Walshire, L., Taylor, O.-D., & Berry, W. (2019). *Laboratory measure of SWCC for a poorly graded fine sand*. Engineer Research and Development Center (U.S.). https://doi.org/10.21079/11681/33676

Witczak, M., Andrei, D., & Houston, W. (2000). *Resilient modulus as function of soil moisture–summary of predictive models. Development of the 2002 guide for the development of new and rehabilitated pavement structures, NCHRP 1-37 A*. Inter team technical report (Seasonal 1).

Witczak, M., & Uzan, J. (1988). *The universal airport design system, report I of IV: Granular material characterization*. Department of Civil Engineering, University of Maryland, College Park.

Zapata, C. E. (2018). Empirical approach for the use of unsaturated soil mechanics in pavement design. In L. Hoyos, J. S. McCartney, S. L. Houston, & W. J. Likos (Eds.), *Panam unsaturated soils 2017* (pp. 149–173). American Society of Civil Engineers. https://doi.org/10.1061/9780784481677.008

Zapata, C. E., Andrei, D., Witczak, M. W., & Houston, W. N. (2007). Incorporation of environmental effects in pavement design. *Road Materials and Pavement Design*, *8*(4), 667–693. https://doi.org/10.1080/14680629.2007.9690094

Zhang, J., Peng, J., Liu, W., & Lu, W. (2021). Predicting resilient modulus of fine-grained subgrade soils considering relative compaction and matric suction. *Road Materials and Pavement Design*, *22*(3), 703–715. https://doi.org/10.1080/14680629.2019.1651756

Zhang, J., Peng, J., Zheng, J., & Yao, Y. (2020). Characterisation of stress and moisture-dependent resilient behaviour for compacted clays in South China. *Road Materials and Pavement Design*, *21*(1), 262–275. https://doi.org/10.1080/14680629.2018.1481138